CubeSat Control using SDRE Method during the Orbital Injection Phase based on Thrusters

ALESSANDRO GERLINGER ROMERO[1], LUIZ CARLOS GADELHA DE SOUZA[2]

[1]Space Mechanics and Control Division
National Institute for Space Research
São José dos Campos
BRAZIL

[2]Aerospace Department
Federal University of ABC
São Bernardo do Campo
BRAZIL

Abstract: Accurately managing a CubeSat's orientation during the orbital injection phase is crucial for mission success. Concurrently, signal processing is vital for the CubeSat payload and its subsystems, particularly for the Attitude Control Subsystem (ACS). Typically, a CubeSat begins this phase with excessive angular velocity so that the controller needs to slew the CubeSat into small angle attitudes for normal operation mode. Cold gas thrusters are one method to perform this transition. This work applies an ACS algorithm during the orbital injection phase, of nonlinear dynamics behavior as angular velocities are high and perturbed in nature. Consequently, linear control methods may fail to meet performance and robustness requirements. To address this, we employ the State-Dependent Riccati Equation (SDRE) method, which is applicable to these types of nonlinear systems. The SDRE controller uses cold gas thruster torques to execute large-angle maneuvers, reducing high angular velocities. This study verifies the numerical simulator model, the control algorithm's functionality, and the signal between the controller and actuators, applying a full Monte Carlo perturbation model. Although the ACS algorithm is designed as a continuous-time system, it is now prepared for the next study phase, which involves analyzing discretization techniques and evaluating the sampling rate for the digital version of the SDRE controller.

Key-Words: CubeSat, Control, SDRE, Orbital, Injection, Thruster

Received: February 19, 2025. Revised: September 11, 2025. Accepted: September 15, 2025. Published: November 6, 2025.

1 Introduction

Cube-Satellites (CubeSats) are to days experiencing an increasing attention within the space community, spanning academia, industry, and space agencies. As of August 2022, a total of 2068 CubeSats have been launched, including those that failed to launch [1]. The requirements for attitude control in CubeSats have evolved, making propulsion subsystems increasingly common [2, 3]. These propulsion subsystems are essential for orbit maneuvers and attitude control, in particular, for orbital injection.

Accurate attitude control during the orbital injection phase is crucial for mission success. Such a mission phase is particularly critical, demanding the highest actuator performance [4]. Typically, a CubeSat begins this phase with excessive angular velocity so that the controller needs to slew the CubeSat into small angle attitudes for normal operation mode. Cold gas thrusters are one method to perform this transition.

The design of a CubeSat attitude control subsystem (ACS) faces challenges related to plant uncertainties, large angle maneuvers, and rapid attitude regulation under tight pointing requirements, making nonlinear control methods suitable candidates for achieving the desired performance and robustness. As an example, there is the Nano-satellite Constellation for Environmental Data Collection (CONASAT) [5, 6], a set of remote sensing CubeSats from the Brazilian National Institute for Space Research (INPE) in which the ACS must meet the stabilization of the satellite in three axes to enable the reception of data from platforms throughout Brazil.

One nonlinear control method for ACS is the State-Dependent Riccati Equation (SDRE), proposed first in [7] and explained further in [8]. SDRE provides an efficient algorithm for the synthesis of nonlinear feedback control via system state nonlinearities with a design flexibility in terms of the state-dependent weighting matrices. SDRE organizes the system model in terms of state-dependent

coefficient (SDC) matrices to develop a suboptimal control law via online algebraic Riccati equation (ARE) solution. This approach linearizes the plant at each operating point to create a constant state-space model, which is then repeatedly updated at each sampling interval to handle multiple linear models that depend on the current state, derived from an original nonlinear system.

The SDRE method has been regarded as the nonlinear counterpart of the linear-quadratic regulator (LQR) control method [8, 9].

This work applies an ACS algorithm during the orbital injection phase, of nonlinear dynamics behavior as angular velocities are high and perturbed in nature. Linear control methods may not meet performance and robustness requirements, so we evaluate the SDRE method, which can handle such nonlinear systems. The SDRE controller uses cold gas thruster torques for large-angle maneuvers to reduce high angular velocities.

Current work does not explore related topics such as optimal thruster geometry, orbital dynamics [10, 11], and attitude estimation. For a thorough overview of the SDRE method and its systematic use with nonlinear systems is discussed in [8]. The SDRE method has been applied to control nonlinear systems like the six-degree-of-freedom CubeSat model in this work [12, 13]. Additionally, [17] expanded an open-source project to create a simulator. In the case of CONASAT, [6] used SDRE as a filtering technique alongside a PID controller, whilst [17] compared the performance and robustness of SDRE with a PID controller.

The SDRE method and the associated ARE problem have been thoroughly researched, as an example in [14], which explores different approaches for solving the ARE and their resource needs. Despite the intensive resource demands for online ARE solving, SDRE offers simplicity, numerical tractability, and design flexibility, comparable to LQR [15, 16].

To the best of our knowledge, CONASAT is not expected to include inertial actuators [5, 6]. Therefore, this work utilized available CubeSat data extended with a cold gas propulsion subsystem. This approach is consistent with the CubeSat industry's practice of employing inertial actuators during the orbital injection phase.

In order to test the control adequacy, the CubeSat is designed as a continuous-time system for a full Monte Carlo perturbation model. The next study phase involves analyzing discretization techniques and evaluating the sampling rate for the digital SDRE controller [18]. The Monte Carlo perturbation model investigation evaluates the numerical simulator model and verifies the control algorithm's functionality, which is designed using the SDRE controller. It also suggests that SDRE can enhance missions developed by INPE, particularly CONASAT.

The structure of this paper is as follows: Section 2 outlines the SDRE method, Section 3 dives into the CubeSat's physical modeling within the simulator, Section 4 discusses state-space models and controllers, Section 5 presents the simulation results, and Section 6 concludes the study.

2 SDRE

The SDRE method works by breaking down the nonlinear dynamics into a state vector and a matrix-valued function that depends on the state itself. Such an approach converts the nonlinear system into a linear structure with state-dependent coefficient (SDC) matrices, pair (A, B), as Eq. (1).

$$\dot{x} = A(x)x + B(x)u$$
$$y = Cx \tag{1}$$

In Eq. (1), $x \in R^n$ represents the state vector, and $u \in R^m$ represents the control vector. The SDC form resembles the structure of a linear system, but the pair (A, B) is a function of the state vector x. While the non-uniqueness of SDC matrices provides additional flexibility that can enhance controller performance, it also introduces challenges. For instance, not all SDC matrices satisfy the SDRE requirements, such as the need for the pair (A, B) to be pointwise stabilizable.

The system model in Eq. (1) is evaluated under the cost functional in Eq. (2).

$$J(x_0, u) = \frac{1}{2}\int_0^\infty (x^T Q(x)x + u^T R(x)u)dt \tag{2}$$

where $Q(x) \in R^{n\times n}$ and $R(x) \in R^{m\times m}$ are the state-dependent weighting matrices. For local stability, $Q(x)$ must be positive semi-definite, and $R(x)$ must be positive definite [6].

The SDRE controller works by linearizing the plant around the current operating point, generating constant state-space matrices to implement the LQR. This process is repeated at each sampling step, effectively transforming the nonlinear model into a linear one, solving an Algebraic Riccati Equation (ARE), and calculating a proportional gain at each step. Therefore, based on LQR theory applied to Eq. (1) and Eq. (2), the state-feedback control law at each sampling step is given by $u = -K(x)x$, where the state-dependent gain $K(x)$ is:

$$K(x) = R^{-1}(x)B^T(x)P(x) \quad (3)$$

and P(x) is the unique, symmetric, positive definite solution of the ARE expressed as:

$$P(x)A(x) + A^T(x)P(x) - P(x)B(x)R^{-1}(x)B^T(x)P(x) + Q(x) = 0 \quad (4)$$

Since Eq. (4) is solved at each sampling step, it simplifies to an ARE.

3 CubeSat Physical Modeling

The simulator model is crafted based on a standard mission by INPE, where the ACS must stabilize a CubeSat along three axes to ensure its antennas point toward the intended target. Specifically, this work investigates the orbital injection phase of the CONASAT, an 8U CubeSat with a side length of 0.2 meters.

In terms of sensors, there are two primary types of attitude determination hardware: attitude sensors and angular velocity sensors [11]. The simulator includes both types: (1) a set of attitude sensors, such as Sun sensors (commonly used for Earth-orbiting satellites), and (2) an angular velocity sensor, specifically a gyroscope. The sensors in the simulator are simplified, allowing them to measure physical quantities at any moment with complete accuracy and no noise. Furthermore, the Sun sensors continuously deliver the Sun versor measurement in the body-fixed frame throughout the simulation, under the assumptions of no eclipse, a stationary Sun in the Earth-centered inertial (ECI) reference frame, and uninterrupted visibility of the Sun by each sensor. The ECI serves as a quasi-inertial reference frame commonly utilized in ACS.

The following subsections delve into details of relevant CubeSat physical modeling aspects.

3.1 Propulsion Subsystem

To effectively manage attitude control, it is important to explore the various methods available for generating torques. Actuators can be classified into two main categories: (1) inertial actuators - these actuators change the satellite's overall inertial angular momentum by producing external torques, such as those generated by cold gas propulsion subsystems; and (2) momentum exchange actuators - unlike inertial actuators, these do not alter inertial angular momentum.

The most basic cold gas propulsion subsystem comprises a pressurized gas tank and thrusters managed by solenoid valves. Its operation can be summarized as follows: (A) the tank is filled with a highly pressurized gas; (B) the gas flow is controlled by solenoid valves before it reaches the thrusters; and (C) when the solenoid valves are activated, the high-pressure gas expands and accelerates through the nozzle, generating the required thrust.

This streamlined propulsion subsystem design offers lower mass, reduced power consumption, and enhanced durability. However, as the mission advances, the tank pressure diminishes due to propellant consumption, resulting in a decrease in the subsystem's thrust output.

A crucial aspect of designing the propulsion subsystem is selecting the propellant, as it directly influences the choice of both the propellant tank and thrusters. Various gaseous propellants with different specific impulses are available, including helium (GHe), nitrogen (GN2), and xenon (GXe). Due to the low specific impulse of these propellants, the thrust typically ranges between 10mN and 4N.

The cold gas propulsion subsystem is modeled using three pairs of thrusters, each corresponding to a rotation axis: yaw, pitch, and roll. Each pair is mounted on opposite sides of the CubeSat, aligned along the respective axis of inertia, and arranged back-to-back to produce symmetric torques. The external torque is described by Eq. (5).

$$\vec{g_{cm}} = -\sum_{n=1}^{3} \vec{r_n} \times T_n \vec{a_n} \vec{a_n}^T \quad (5)$$

where g_{cm} represents the external torque at the CubeSat's center of mass, T_n denotes the thrust magnitude along the symmetry axis a_n for each pair of opposite nozzles, and r_n is the position vector from the CubeSat's center of mass to the symmetry axis a_n of the nozzles.

Given the characteristics of solenoids, the control mechanism for this type of propulsion subsystem operates in an ON-OFF manner, resulting in impulsive control [19].

3.2 Rotational Kinematics

Considering the inertial reference frame F_i and the body reference frame F_b with its origin at the CubeSat's center of mass, the CubeSat's attitude can be defined by a rotation matrix denoted by a unit quaternion $Q = [q_1\ q_2\ q_3 \mid q_4]^T$. The CubeSat's angular velocity is defined as $\omega = [\omega_1\ \omega_2\ \omega_3]^T$. Therefore, the kinematics can be modeled using the Gibbs vector $Q = [g \mid q_4]$, as shown in Eq. (6).

$$\dot{Q} = -\frac{1}{2}\begin{bmatrix}\omega^{\times}\\ \omega^{T}\end{bmatrix}\begin{bmatrix}q_1\\ q_2\\ q_3\end{bmatrix} + \frac{1}{2}q_4\begin{bmatrix}1_{3\times 3}\\ 0\end{bmatrix}\omega \tag{6}$$

where $\omega^{\times}$ represents the skew-symmetric matrix and *1* denotes the identity matrix.

3.3 Rotational Mechanics

To analyze the variations in angular velocity, it is mandatory to study the changes in the CubeSat's angular acceleration. According to the Euler-Newton equations for rotational mechanics, angular acceleration is generated by torques. In other words, the rate of change of angular momentum $\vec{\mathrm{h}}$ is equal to the net torques $\vec{\mathrm{g}}$ acting on the CubeSat, as shown in Eq. (7). As a disclaimer, the rotational mechanics is derived based on the CubeSat's center of mass; for the general case, refer to [10].

$$\vec{\mathrm{h}} = \vec{\mathrm{g}} \tag{7}$$

Considering the motion of the body-fixed frame F_b relative to the ECI frame F_i and the angular velocity ω, the rate of change of angular momentum in F_b is given by Eq. (8).

$$\vec{h} = \vec{g} - \vec{\omega} \times \vec{\mathrm{h}} \tag{8}$$

Moreover, $\vec{h} = \mathrm{I}.\vec{\omega}$ and $\vec{h} = \mathrm{I}.\vec{\omega}$, in which I is the time-invariant inertia tensor. Combining this definition with Eq. (8) results in Eq. (9).

$$\mathrm{I}.\vec{\omega} = \vec{\mathrm{g}} - \vec{\omega} \times (\mathrm{I}.\vec{\omega}) \tag{9}$$

The CubeSat is equipped with three pairs of thrusters, each aligned with its principal axes of inertia. These thrusters act as inertial actuators, producing external torques. Consequently, the CubeSat's rotational mechanics is governed by Eq. (10).

$$\dot{\omega} = \mathrm{I}^{-1}\mathrm{g}_{\mathrm{cm}} - \mathrm{I}^{-1}\omega^{\times}\mathrm{I}\omega \tag{10}$$

where g_{cm} represents the external torque produced by the cold gas thrusters.

4 Controller Design

The model of CubeSat is designed to maintain total angular momentum close to zero, requiring control over two dynamic states: (1) the attitude, which can be described by unit quaternions Q, and (2) its stability $\dot{Q}$, indeed, the angular velocity ω of the CubeSat. For that reason, the following high-level requirements were refined: (1) "the attitude must be stabilized and must align with the Sun based on a specified Sun versor within the CubeSat", and (2) "the angular velocities measured by the gyroscope should be minimized as much as possible". These requirements are common during the orbital injection phase, often regarded as the most critical stage of a mission, requiring maximum actuator performance [4].

Considering Eq. (1), the state and the control vectors are represented in accordance with Eq. (11).

$$\begin{bmatrix}x_1\\ x_2\end{bmatrix} = \begin{bmatrix}Q\\ \omega\end{bmatrix}$$
$$\begin{bmatrix}u_1\end{bmatrix} = \begin{bmatrix}T_c = g_{cm}\end{bmatrix} \tag{11}$$

The stabilization problem involves determining errors in both attitude (x_1) and angular velocity (x_2). The error of the angular velocity is straightforwardly obtained from gyroscope data, while the error of the attitude must be computed. Regarding the attitude error, it is determined by computing a rotation, represented by a unit quaternion Q, required to align the actual Sun versor (in the CubeSat frame) with the reference versor in the CubeSat frame.

The upcoming subsection delves into the SDRE controller. Table 1 outlines the CubeSat specifications [5, 6] and references utilized in the simulation results presented in Section 5.

4.1 SDRE Controller

In slow-paced maneuvers, a linear controller is appropriate and commonly utilized. However, during maneuvers required in the orbital injection phase, linearized equations become insufficient, and discontinuities may destabilize the system (e.g., impulsive torques from actuators that do not allow intermediate control torques). To overcome the limitations of linearization, the SDRE method is employed [20].

The SDRE method entails restructuring the system model into a pseudo-linear form, as defined by Eq. (1), and subsequently solving an ARE at each sampling step.

If the net external torques g_{cm} are exclusively generated by the cold gas propulsion subsystem, the rotational mechanics is governed by Eq. (10). Furthermore, considering the vectors specified in Eq.

(11), the state space model is derived using Eqs. (6) and (10), leading to Eq. (12).

$$\begin{bmatrix}\dot{x_1}\\ \dot{x_2}\end{bmatrix} = \begin{bmatrix} -\frac{1}{2}\begin{bmatrix}\omega^{\times}\\ \omega^{T}\end{bmatrix} & 0 & \begin{bmatrix}\frac{1}{2}q_4 I_{3\times 3}\\ 0\end{bmatrix} \\ 0 & 0 & -I^{-1}\omega^{\times} I \end{bmatrix} \begin{bmatrix}x_1\\ x_2\end{bmatrix} + \begin{bmatrix}0\\ I^{-1}\end{bmatrix}\begin{bmatrix}u_1\end{bmatrix}$$

$$\begin{bmatrix}y\end{bmatrix} = 1\begin{bmatrix}x_1\\ x_2\end{bmatrix} \quad (12)$$

Eq. (12) has been shown to meet the conditions for SDRE. Consequently, the state-dependent gain K is calculated using Eq. (3), which then facilitates the computation of the control vector $\overrightarrow{u_1} = -K(\vec{x})\vec{x}$.

5 Simulation Results

A simulation test was performed using a comprehensive Monte Carlo perturbation model, detailed as follows: (1) the initial Euler angle errors of the CubeSat were obtained from three independent uniform distributions: $X : U(-180.0, 180.0)$, $Y : U(-90.0, 90.0)$, $Z : U(-180.0, 180.0)$ degrees; and (2) the initial angular velocity errors were sampled from three independent uniform distributions: $X : U(-0.1, 0.1)$, $Y : U(-0.1, 0.1)$, $Z : U(-0.1, 0.1)$ rad/s. The Monte Carlo model was executed 15 times, with a simulation duration of 1000 seconds, a fixed step of 0.1 seconds, and the data presented in Table 1. The SDRE controller was defined by Eq. (12) using constant weighting matrices $R = 1$ and $Q = 1$ (1 denoting the identity matrix).

Fig. 1 depicts the set of all quaternion errors calculated throughout the simulations. Notably, the scalar part of the quaternions (q_4) converged over time to ±1 ($q_4 \rightarrow \pm 1$), while the vector component of the quaternion approached zero ($[q_1\ q_2\ q_3]^T \rightarrow [0\ 0\ 0]^T$). This convergence demonstrates that the CubeSat successfully achieved its target attitude in all simulation runs. However, due to the impulsive control applied, there was a steady-state error, rendering the system marginally stable.

Regarding the CubeSat angular velocities, Fig. 2 displays the respective collection of angular velocities for each axis. The angular velocities approached zero ($[X\ Y\ Z]^T \rightarrow [0\ 0\ 0]^T$) rad/s, signifying that the reference angular velocities were achieved in all runs. Again, due to the cold gas propulsion subsystem, there was an error, making the system marginally stable.

TABLE 1 – CUBESAT'S SPECIFICATIONS AND REFERENCES

Name	Value
Specifications	
unit	8U
size (m)	[0.2 0.2 0.2] ^{T}
mass (kg)	8.2
inertia tensor (kg.m^2)	$\begin{bmatrix}0.0547 & 0 & 0\\ 0 & 0.0519 & 0\\ 0 & 0 & 0.0574\end{bmatrix}$
thrust (mN)	10
References	
Solar vector (XYZ)	[1 0 0] ^{T}
Angular velocity (rad/s)	[0 0 0] ^{T}

Figure 3 shows the torques from the cold gas propulsion subsystem for each axis, confirming the system's marginal stability due to its periodic nature. Torques were periodically required to maintain the target attitude and angular velocities.

All torques had the same magnitude (10mN × 0.1 meters = 1mN.m), and their frequency decreased over time, indicating a periodic system. These simulation results do not apply to general scenarios or initial conditions beyond the range defined by the Monte Carlo perturbation model, owing to the inherent nonlinear phenomena.

6 Conclusion

To the best of our knowledge, CONASAT is not expected to include inertial actuators [5, 6]. Therefore, this work utilized available CubeSat data extended with a cold gas propulsion subsystem. This approach is consistent with the CubeSat industry's practice of employing inertial actuators during the orbital injection phase.

In the context of assessing whether the application of the SDRE method in ACS could enhance INPE's missions, the performance during the orbital injection phase is critical for ensuring mission success. So, based on the simulation results, which demonstrate that the SDRE controller can meet the requirements,

there is evidence that SDRE can indeed offer benefits. Nonetheless, SDRE controllers demand greater computing resources and often pose verification challenges. As a result, drawing a definitive conclusion at this stage remains premature.

In this study, the SDRE controller was designed as a continuous-time system to enable a comprehensive Monte Carlo perturbation model, which was used to test the adequacy of the control method. The next phase of this research involves analyzing discretization techniques, where the sampling rate for the digital version of the SDRE controller will be evaluated.

In summary, the use of inertial actuators for CubeSat control is a growing trend. At the same time, simulation outcomes suggest that the SDRE method has the potential to enhance the performance of INPE's CubeSat missions, in particular, CONASAT. Nevertheless, further research is needed to address verification challenges, focusing on the a priori assessment of the resulting marginal stability.

Fig. 1. The quaternion errors of the CubeSat during the simulation test performed using the Monte Carlo perturbation model.

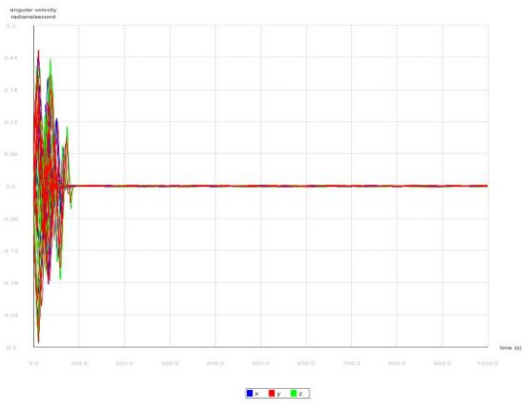

Fig. 2. The angular velocities of the CubeSat during the simulation test performed using the Monte Carlo perturbation model.

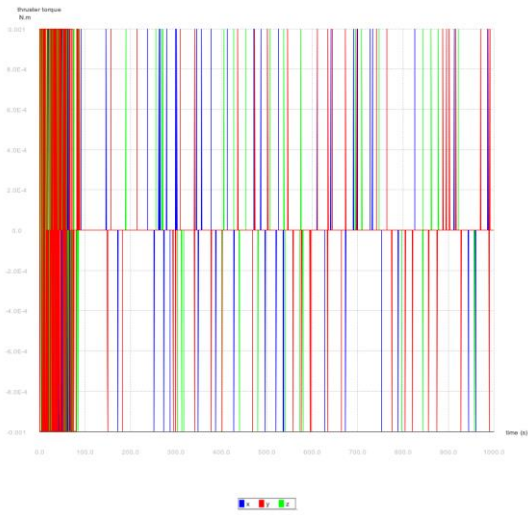

Fig. 3. The thrusters' torques of the CubeSat during the simulation test performed using the Monte Carlo perturbation model.

References:

[1] Kulu, E., "Nanosatellite Launch Forecasts 2022: Track Record and Latest Prediction," Proceedings of the 36th Annual Small Satellite Conference, 2022.

[2] Tummala, A. R., and Dutta, A., "An Overview of Cube-Satellite Propulsion Technologies and Trends," Aerospace, Vol. 4, No. 4, 2017. doi:10.3390/aerospace4040058, URL https://www.mdpi.com/2226-4310/4/4/58.

[3] Lemmer, K., "Propulsion for CubeSats," Acta Astronautica, Vol. 134, 2017, pp. 231–243. doi:https://doi.org/10.1016/j.actaastro. 2017.01.048.

[4] Wertz, J. R., and Larson, W. J., Space Mission Analysis and Design, Springer Dordrecht, 1999.

[5] de Carvalho, M. J. M., "Estudo de uma Missão Espacial para Coleta de Dados Ambientais Baseada em Nano Satélites,", 2010. URL http://www.crn.inpe.br/conasat1/Satélites.pdf, access date: 21. Oct.2018.

[6] B. D. Reis de Mesquita and H. Koiti Kuga and V. Carrara, "Estimation and Attitude Control in CONASAT Nominal Operation Mode: An Approach for SDRE Filter and PID Control," IEEE Latin America Transactions, Vol. 15, No. 5, 2017, pp. 835–842.

[7] Pearson, J.D., "Approximation Methods in Optimal Control", Journal of Electronics and Control, Vol.13, No. 5, 1962, pp. 453–469. doi:10.1080/00207216208937454, URL https://doi.org/10.1080/00207216208937454.

[8] Çimen, T., "Systematic and effective design of nonlinear feedback controllers via the state-

dependent Riccati equation (SDRE) method," Annual Reviews in Control, Vol. 34, No. 1, 2010,pp.32–51. doi:10.1016/j.arcontrol.2010.03.001.

[9] Cloutier, J. R., D'Souza, C. N., and Mracek, C. P., "Nonlinear regulation and nonlinear H-infinity control via the state-dependent Riccati equation technique." Conference on Nonlinear Problems in Aviation, No. September, 1996.

[10] Hughes, P. C., Spacecraft Attitude Dynamics, New York, 1986.

[11] Sidi, M. J., Spacecraft Dynamics and Control - A Practical Engineering Approach, Cambridge University press, 2006.

[12] Gonzales, R. G., and Souza, L. C. G. d., "Application of the SDRE Method to Design an Attitude Control System Simulator," Advances in the Astronautical Sciences, Vol. 134, No. Part 1-3, 2009, pp. 2251–2258. INPE

[13] Stansbery, D. T., and Cloutier, J. R., "Position and attitude control of a spacecraft using the state-dependent Riccati equation technique," Proceedings of the 2000 American Control Conference. ACC (IEEE Cat. No.00CH36334), Vol. 3, 2000, pp. 1867–1871 vol.3. doi:10.1109/ACC.2000.879525.

[14] Romero, Alessandro Gerlinger; Souza, Luiz Carlos Gadelha. An Approach to Evaluate the Region of Attraction of Satellites Controlled by SDRE. WSEAS TRANSACTIONS ON SYSTEMS, v. 21, p. 75-85, 2022.

[15] Di Mauro, G., Schlotterer, M., Theil, S., and Lavagna, M., "Nonlinear Control for Proximity Operations Based on Differential Algebra," Journal of Guidance, Control, and Dynamics, Vol. 38, No. 11, 2015, pp. 2173–2187. doi:10.2514/1.G000842, URL https://doi.org/10.2514/1.G000842.

[16] Di Mauro, G., Di Lizia, P., and Lavagna, M., "Control of Relative Motion via State-Dependent Riccati Equation Technique," AAS/IAAA. Astrodynamics Specialist Conference, Vol 142, Univelt, San Diego, Ca, 2011.

[17] Romero, A. G., and Souza, L. C. G. d., "State-dependent Riccati equation controller using Java in remote sensing CubeSats," Journal of Applied Remote Sensing, Vol. 13, No. 3, 2019, p. e032509. doi:10.1117/1.JRS.13.032509, URL http://dx.doi. org/10.1117/1.JRS.13.032509.

[18] Adrielle C. Santana et al., "Attitude Control of a Satellite by Using Digital Signal Processing" Journal of Aerospace Technology and Management, vol. 4, no.1, 2012, pp. 15-24 Brasil

[19] Yang, T., "Practical Stability of Impulsive Control," Impulsive Control Theory, Springer Berlin Heidelberg, Berlin, Heidelberg, 2001, pp. 149–197.

[20] Fortescue, P. W., and Swinerd, G. G., "Attitude Control," Spacecraft Systems Engineering, No. June, 2011, pp. 289–326. doi:10.1002/9781119971009.ch9, URL http://doi.wiley.com/10.1002/9781119971009.ch9.

Contribution of Individual Authors to the Creation of a Scientific Article (Ghostwriting Policy)

Both authors equally contributed to the present research, at all stages from the formulation of the problem to the final findings and solution. Moreover, Dr. Alessandro G Romero carried out the simulation of the ACS, and Dr. Luiz Carlos G Souza was responsible for the derivation of the dynamics of the satellite.

Sources of Funding for Research Presented in a Scientific Article or Scientific Article Itself

No funding was received for conducting this study.

Conflict of Interest

The authors have no conflicts of interest to declare that are relevant to the content of this article.